



## Molecular Crystals and Liquid Crystals Science and Technology. Section A. Molecular Crystals and Liquid Crystals

Publication details, including instructions for authors and  
subscription information:

<http://www.tandfonline.com/loi/gmcl19>

### Diffuse Scattering in Disordered Molecular Crystals

T. R. Welberry<sup>a</sup> & R. L. Withers<sup>a</sup>

<sup>a</sup> Research School of Chemistry, Australian National University,  
Canberra, ACT 2601, Australia

Version of record first published: 27 Oct 2006.

To cite this article: T. R. Welberry & R. L. Withers (1992): Diffuse Scattering in Disordered Molecular Crystals, Molecular Crystals and Liquid Crystals Science and Technology. Section A. Molecular Crystals and Liquid Crystals, 211:1, 17-33

To link to this article: <http://dx.doi.org/10.1080/10587259208025801>

PLEASE SCROLL DOWN FOR ARTICLE

Full terms and conditions of use: <http://www.tandfonline.com/page/terms-and-conditions>

This article may be used for research, teaching, and private study purposes. Any substantial or systematic reproduction, redistribution, reselling, loan, sub-licensing, systematic supply, or distribution in any form to anyone is expressly forbidden.

The publisher does not give any warranty express or implied or make any representation that the contents will be complete or accurate or up to date. The accuracy of any instructions, formulae, and drug doses should be independently verified with primary sources. The publisher shall not be liable for any loss, actions, claims, proceedings, demand, or costs or damages whatsoever or howsoever caused arising directly or indirectly in connection with or arising out of the use of this material.

## DIFFUSE SCATTERING IN DISORDERED MOLECULAR CRYSTALS

T.R.WELBERRY & R.L.WITHERS

Research School of Chemistry, Australian National University,  
Canberra, ACT 2601, Australia.

(Received July 12, 1991)

**Abstract** Conventional crystal structure analysis using Bragg diffraction data reveals only average one-body structural information, such as atomic positions, thermal ellipsoids and site occupancies. Diffuse scattering, on the other hand, gives two-body information and is thus potentially a rich source of information of how molecules interact. However, since typical diffuse scattering intensities are  $\sim 10^3$ - $10^4$  down on Bragg intensities, obtaining such information is still a far from routine process and quantitative studies are rare. In this paper we describe some of the concepts and difficulties involved, with particular reference to the example of 1,3-dibromo-2,5-diethyl-4,6-dimethyl benzene (BEMB2), which is disordered as a result of the fact that the molecule can take up either one of two different orientations in a given molecular site.

**Keywords:** *diffuse scattering, disorder, molecular crystal, molecular packing, position-sensitive detector*

### INTRODUCTION

For some years we have been interested in disordered molecular crystals in which the disorder arises because the molecule is able to take up either one of two different orientations in a given molecular site. In particular we have concentrated on aromatic systems in which a simple  $180^\circ$  rotation of the molecule effectively results in the interchange of halogen (Br- or Cl-) and methyl-substituents. Because the packing volumes of these three groups are so similar, the molecule can pack into a given molecular site in the crystal in these two different orientations with very little difference ( $\sim kT$ ) in energy. In such a situation disorder is guaranteed, but because there are small differences in energy the distribution of the two different orientations will not be random:

- i.e short range order will occur. We have only been interested in systems in which the disorder occurs at growth and once the molecule forms part of the bulk, the barrier to reorientation is so high that the disorder is effectively *locked-in*. Examples of the molecular systems we have studied<sup>1,2,3,4,5</sup> are shown in Figure 1. Our aim has been to measure the diffuse X-ray diffraction patterns from these compounds and attempt to explain them in terms of a detailed description of how the molecules interact with each other.

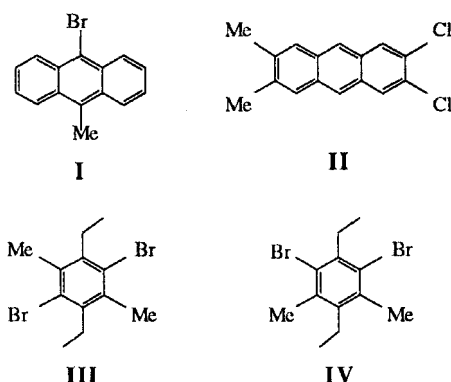


FIGURE 1. Molecules forming disordered crystals in which each molecular site is occupied by the molecule in one of two possible orientations. (I) 9-bromo,10-methylantracene. (II) 2,3-dichloro-6,7-dimethylantracene. (III) 1,4-dibromo-2,5-diethyl-3,6-dimethyl benzene (BEMB1). (IV) 1,3-dibromo-2,5-diethyl-4,6-dimethylbenzene (BEMB2).

Diffuse X-ray scattering intensities from such systems are typically  $\sim 10^3$ - $10^4$  down on the Bragg peak intensities from which conventional crystal structure determination is carried out. This has meant that only relatively recently has it been possible to make extensive quantitative measurements of diffuse scattering, and many studies have been only qualitative or at best semi-quantitative. In experiments our original film-based methods have been replaced by the use of a position-sensitive detector system<sup>6</sup>, which provides quantitative diffuse scattering data with a sensitivity approximately 50 times that obtainable with a single

counter. Although these data are recorded in digital form we still find it invaluable for interpretation to display the information pictorially, first on a computer screen and subsequently in hard copy via an Optronics film-writing device. Two examples of the data from whole reciprocal lattice sections, which we can now obtain routinely, are displayed in Figure 2. It should also be mentioned that these examples were obtained at low temperature (100K) - not a trivial matter when it is imperative the main X-ray beam does not intercept any shielding material.

#### CORRELATION DESCRIPTION OF DISORDER

The intensity scattered at a reciprocal wave-vector  $\underline{S}$  by a two component substitutionally disordered crystal may be expressed as<sup>2,3,7</sup>,

$$I(\underline{S}) = N \left| \left( m_A F_n^{(A)} + m_B F_m^{(B)} \right) \sum_n^{\text{cell}} \exp(2\pi i \underline{S} \cdot \underline{R}_n) \right|^2 \\ + N m_A m_B \Delta F_n \Delta F_m^* \sum_n^{\text{cell}} \sum_m C_{nm}^{AB} \exp(2\pi i \underline{S} \cdot \underline{R}_{nm}) \quad (1)$$

Here  $F_n^{(A)}$  is the scattering factor for an A-type molecule at site  $n$ , specified by the vector  $\underline{R}_n$ ;  $\underline{R}_{nm} = \underline{R}_n - \underline{R}_m$ ;  $\Delta F_n = F_n^{(A)} - F_n^{(B)}$ ;  $m_A$  and  $m_B$  are the concentrations of the two species A and B and  $C_{nm}$  is a correlation coefficient which is related to the joint probability  $P_{nm}^{AA}$  that two molecular sites  $n$  and  $m$  are both occupied by an A molecule.

$$C_{nm} = \frac{P_{nm}^{AA} - m_A^2}{m_A m_B} \quad (2)$$

The first term in (1) represents the Bragg peak intensities and can be seen to be proportional to the average of the molecular scattering factors. The second term is a diffuse scattering term and is seen to be proportional to the *difference* in the molecular

scattering factors. It consists of the sum of many individual terms, each involving a different correlation coefficient  $C_{nm}$ . The origin term in this series corresponds to the case where all  $C_{nm} = 0$ , i.e. the scattering for a *random distribution* of the two species A and B.

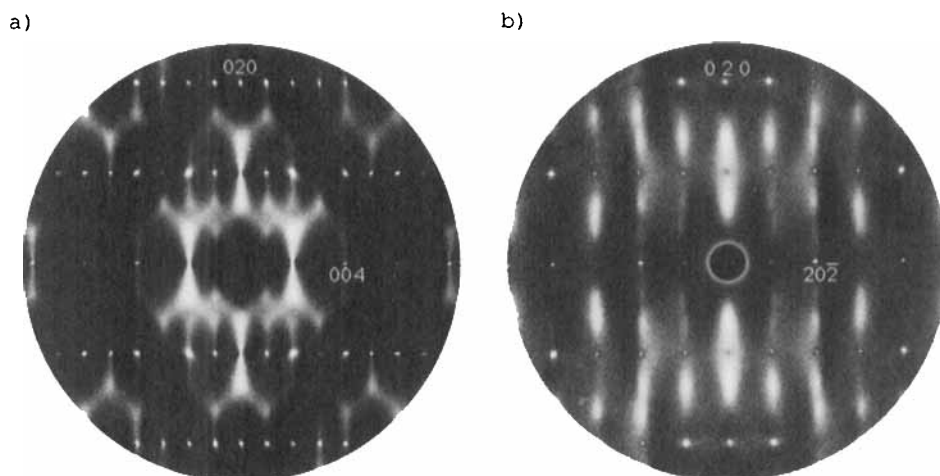


FIGURE 2. Observed diffuse X-ray scattering patterns for BEMB2 at 100K. a) The  $0kl$  section. b) the  $hk-h$  section. The maximum diffraction angle shown is  $2\theta=51.2^\circ$ .

It should be noted that conventional crystal structure analysis using the Bragg intensities (the first term in (1)) reveals the average atomic positions and the site occupancies  $m_A$  and  $m_B$ . Consequently the only unknowns in the diffuse scattering term are the correlation coefficients,  $C_{nm}$ . The form of the contribution for each  $C_{nm}$ , which we call a *correlation distribution*, may be calculated from a knowledge of the average structure, but the magnitude must be determined. In Figure 3 we show examples of such calculated correlation distributions for the case of the  $(hk-h)$  section of 1,3-dibromo-2,5-diethyl-4,6-dimethylbenzene (BEMB2), the observed diffuse scattering for which is shown in Figure 2b. We have developed a least-squares procedure

which adjusts the values of the coefficients  $C_{nm}$  for distributions corresponding to intermolecular vectors within a certain radius of a given molecule, to obtain the best fit to the observed data.

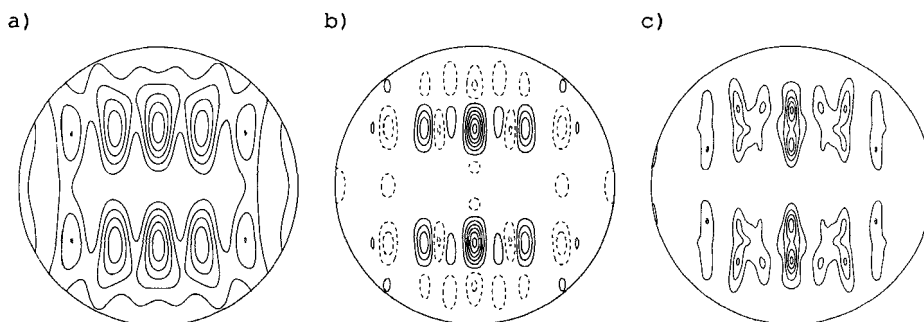


FIGURE 3. Calculated distributions for the  $h\ k\ -h$  section of BEMB2. a) The intensity for a random distribution of A and B orientations. b) The correlation distribution corresponding to the site 65501. c) The total calculated intensity - cf. Figure 2b.

We use the ORTEP method of labelling molecular sites<sup>8</sup>, where for example 55501 refers to a central molecule, 55502 to a second symmetry-related site in the same cell, and for sites related by cell translations the first three digits increase or decrease accordingly. In an analysis it is quite feasible to fit ~50 such functions to the observed data. The determined coefficients correspond to inter-molecular vectors within a few molecular shells of a central molecule (molecules whose centres are within ~20Å). It should be noted that symmetry-related vectors are assumed to have the same  $C_{nm}$  value. In Table 1 we show some results for the strongest correlations obtained for BEMB2. Of 42 unique correlation coefficients measured, all others had absolute values less than 0.10.

TABLE 1. Contact types and intermolecular distances for BEMB2 refer to a structure in which all molecules are in orientation A. Distances are calculated using the coordinates of the composite disordered atoms obtained from the average crystal structure determination. Contacts are from a central molecule at site 55501.

Site	$C_{nm}$	Intermolecular Contact
65501	0.21	Me-Br 4.08 Å Me-Me, Br-Br 3.90 Å
66502	0.14	Br-Me 4.29 Å
64501	-0.12	-
66501	-0.10	Me-Br 4.08 Å
56501	-0.10	Me-Br, Me-Br 3.90 Å Me-Me, Br-Br 4.44 Å

Several points of note arise out of these results. First, it is clear that the order is only very short range in this compound. For other compounds such as I and II (see Figure 1) much higher values of  $C_{nm}$  have been observed. However, even such small degrees of order are easily detectable and produce scattering patterns easily distinguishable from the random pattern. As we have found for other compounds the most significant ordering occurs between molecules which have a direct intermolecular contact involving the disordered atomic sites. That is to say, a contact which is directly affected by the interchange of the Br and methyl groups that occurs if the neighbouring molecule is flipped. Consider the contact with the molecule at 66502. A positive value for  $C_{nm}$  means that the proportion of contacts that are Br-Me is increased relative to a purely random distribution. For this contact, and since  $m_A = 0.5$ , a correlation of 0.14 means that there are 28.5% of contacts of the type Br-Me, 28.5% of Me-Br, and 21.5% each of Me-Me and Br-Br. Such a preference for Br's to try to avoid each other is consistent with our findings in other compounds, and may qualitatively be explained in terms of the interactions between

local-dipoles.

The contact with the molecule at 65501, however, is not as simple. As may be seen in Figure 4, there are three different contacts between disordered atomic sites. A positive correlation here implies that for the 4.08Å contact the proportion of Me-Br and Br-Me vectors is increased, but for the two shorter (3.90Å) contacts the proportion of Me-Me and Br-Br vectors is increased. Even if we take account of the direction of the local dipoles K, L, M and N in Figure 4, there appears no good reason why this correlation should be positive.

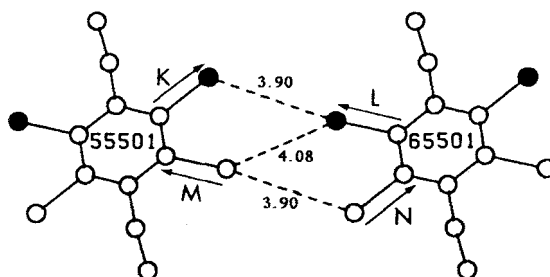


FIGURE 4. The contact between a central molecule (55501) and the molecule (65501) with both in the A orientation. Filled circles represent Br and open circles C. Arrows indicate the local dipoles used to try to account for the short-range ordering

What has gone wrong? Why are we unable to explain even qualitatively what is observed? There are a number of possibilities. First, our analysis assumed the average crystal structure was  $P2_1/c$  whereas the weak presence of some ( $h\ 0\ l$ ,  $l$  odd) Bragg peaks clearly shows the average structure has the space group  $P2_1$ . This means that each of our correlation functions used in the analysis was in fact the sum of two very similar distributions and the determined values of  $C_{nm}$  were the average of two perhaps quite different values. Secondly, the formulation given in equation (1) is only the first approximation to the



scattering from a disordered crystal and assumes that the molecules occur in either one or other orientation in the molecular site and neglects the possibility of local relaxation, which could substantially alter the important intermolecular contact distances mentioned above. It might be noted that in alloys it is well known that local displacements of atoms from their ideal lattice sites may be up to ~5% of the cell spacing. Molecules have the freedom not only to relax by shifts from their mean lattice sites, but also have the freedom to assume slightly different orientations. We are currently attempting to incorporate the possibility of these effects into our analysis since it is clear that the level of agreement ( $R \sim 20\%$ ) we currently obtain for the simple model (1) means that more information is present in our data that is not yet being modelled correctly.

Of particular note in the case of BEMB2 is the fact that the X-ray diffraction patterns shown in Figure 2 contain some features that are not modelled at all by our correlation fitting approach. In the  $0kl$  section the diffuse scattering is generally quite diffuse, consistent with the low values of correlation that were determined. But in the neighbourhood of some lattice peaks, in particular the  $002$  and  $010$  Bragg positions, the scattering peak becomes very narrow, indicative of a range of order far greater than the  $20\text{\AA}$  range that was included in the analysis. This same feature appears also in the  $h k -h$ , section which is approximately normal to  $0kl$ , as a dark 'hole' in the diffuse scattering. This is seen most clearly around the  $010$  Bragg position, since the Bragg peak is systematically absent because of the  $2_1$  symmetry. The width of this hole corresponds to distances in real space in excess of  $\sim 200\text{\AA}$ . In order to understand what is causing these effects we adopt a quite different approach to the analysis of diffuse scattering.

MODULATION WAVE DESCRIPTION OF DISORDER

As we saw above, the intensities of the Bragg peaks in a disordered crystal correspond to the diffraction from the average lattice, and if we had an average lattice then there would be no diffuse scattering. Conversely, we can consider that the intensity at any point in the diffuse scattering at a wave-vector  $\underline{Q} + \underline{k}$ , where  $\underline{Q}$  is a reciprocal lattice vector, is due to a perturbation of this average real-space structure by a periodic modulation characterized by the wave-vector  $\underline{k}$ . For the case of concentration waves these perturbations can be written in the form of a variation from cell to cell of the atomic scattering factors  $f_\mu$ , where  $\mu$  specifies an atomic site within the average unit cell<sup>9,10,11</sup>. The scattering factor appropriate to the  $\mu$ th atom in the cell at the real-space lattice vector  $\underline{R}$  is obtained by summation over all wave-vectors  $\underline{k}$ :-

$$f_\mu(\underline{R}) = \langle f_\mu \rangle \left\{ 1 + \sum_{\underline{k}} \left[ a_\mu(\underline{k}) \exp(2\pi i \underline{k} \cdot \underline{R}) + a_\mu^*(\underline{k}) \exp(-2\pi i \underline{k} \cdot \underline{R}) \right] \right\} \quad (3)$$

Thus a general compositional modulation is characterized by the wave-vector  $\underline{k}$  and the compositional eigenvector  $A(\underline{k}) = (a_1, a_2, \dots, a_\mu, \dots)$ , where  $a_1, a_2$ , etc. are complex. The relationship between the  $a_\mu(\underline{k})$ 's of symmetry-related sites will not in general be random but will reflect the energetics of the particular system under consideration. For modulation wave-vectors along certain high symmetry directions of a parent structure, the lowest energy compositional (and/or displacive) modulations must necessarily transform according to a specific irreducible representation of the little co-group of the corresponding modulation wave-vector (see for example reference 11). If this lowest energy irreducible representation is the only one with a finite amplitude, as is often the case, then the relationship between the  $a_\mu(\underline{k})$ 's of sites related by symmetry operations belonging to the little group of  $\underline{k}$  is fixed by the symmetry of the appropriate irreducible

representation.

As a particularly simple example, suppose we have a structure consisting of 2 symmetry-related atomic sites  $\mu=1$  at  $(0,0,0)$  and  $\mu=2$  at  $(0,1/2,1/2)$  which are occupied with equal probability by either of two different types of atom, A and B, whose scattering factors are  $f_A$  and  $f_B$  respectively. For waves travelling along certain directions, and under the assumption that only the lowest energy irreducible representation is substantially excited, the phase relationship between  $a_1(\mathbf{k})$  and  $a_2(\mathbf{k})$  is fixed by symmetry. For example, if we assume a screw axis along  $\mathbf{b}$ , i.e.  $\{C_{2y}|1/2(\mathbf{b}+\mathbf{c})\}$ , then for modulation wave-vectors along  $\mathbf{b}^*$  the lowest energy modulation must transform according to one or other of the two irreducible representations shown in the following character table:-

	E	$C_{2y}$
$\Sigma_1$	1	1
$\Sigma_2$	1	-1

Then from standard group-theoretical considerations (see for example reference 11),

$$a_2(\mathbf{k}) = a_1(\mathbf{k}) \exp\left[2\pi i \mathbf{k} \cdot \frac{1}{2}(\mathbf{b}+\mathbf{c})\right] \chi^{\Sigma_2}(C_{2y}) \quad (4)$$

For a  $\Sigma_1$  irreducible representation  $\chi(C_{2y}) = +1$  and for a  $\Sigma_2$  irreducible representation  $\chi(C_{2y}) = -1$ . Of course  $\Sigma_1$  and  $\Sigma_2$  strictly only exist for wave-vectors along  $\mathbf{b}^*$ . As soon as  $\mathbf{k}$  moves even slightly away from the  $\mathbf{b}^*$  direction, the corresponding little co-group (see Bradley & Cracknell, 1972) is reduced to a single element - namely the identity E. Thus, on symmetry grounds alone, one can technically no longer relate  $a_2(\mathbf{k})$  to  $a_1(\mathbf{k})$  for the lowest energy modulation. Common sense, however, dictates that the relationship given by equation (4) above should, in most cases, change only slowly as a function of  $\mathbf{k}$ . For a general wavevector we assume that  $\chi(C_{2y}) = \exp[i\theta]$ . Then,

$$a_2(\underline{k}) = a_1(\underline{k}) \exp\left[2\pi i \underline{k} \cdot \frac{1}{2}(\underline{b} + \underline{c})\right] \exp(i\theta) \quad (5)$$

For  $\theta=0$  the modulation is equivalent to the  $\Sigma_1$  irreducible representation and for  $\theta=\pi$  it is equivalent to the  $\Sigma_2$  irreducible representation. For an arbitrary phase,  $\theta$ , it is equivalent to a linear combination of the two.

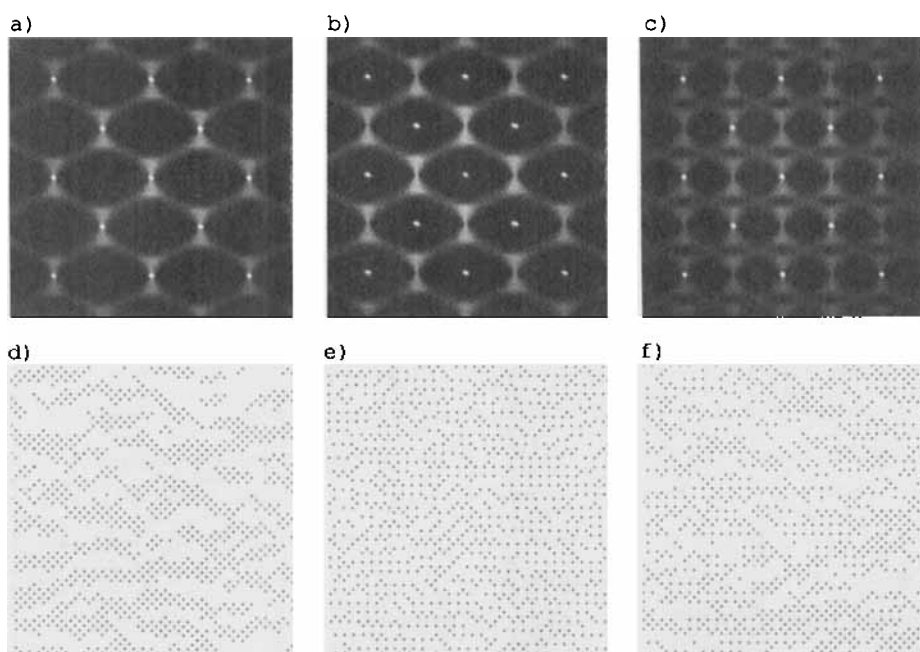


FIGURE 5. Optical diffraction patterns and their corresponding diffraction masks illustrating the two irreducible representations  $\Sigma_1$  and  $\Sigma_2$  described in the text. 5a,d show  $\Sigma_1$ . 5b,e show  $\Sigma_2$ . 5c,f show mixed  $\Sigma_1/\Sigma_2$ .

To demonstrate the meaning of these two different modulations we can make a computer generated model and use optical diffraction to obtain the diffraction pattern. In the examples shown in Figure 5 we have perturbed a simple square lattice, consisting of atoms  $\mu=1$  at  $(0,0,0)$  and  $\mu=2$  at  $(0,1/2,1/2)$ , by a large number of modulations having the two different symmetries  $\Sigma_1$  and  $\Sigma_2$ . In

Figure 5a the modulations all had the  $\Sigma_1$  symmetry, in Figure 5b the modulations all had the  $\Sigma_2$  symmetry and in Figure 5c the modulations were mixed  $\Sigma_1/\Sigma_2$ . The amplitudes of the modulations were chosen to produce a characteristic 'Y' shape of intensity in the first Brillouin zone (for reasons which will become apparent in what follows). The lattice realizations in Figures 5d,e,f corresponding to these diffraction patterns show clearly the meaning of the two different types of mode. For  $\Sigma_1$  the 'Y-shaped' scattering occurs around the Bragg peaks and this gives rise to clusters of atoms which are all black or all white. For  $\Sigma_2$  the 'Y-shaped' scattering occurs between the Bragg peaks and this gives rise to a tendency for black and white to alternate in the [11] direction.

Now let us apply the same techniques to the molecular crystal example of BEMB2. Projected down the  $a$ -axis the structure has molecules  $\mu=1$  at (0,0,0) and  $\mu=2$  at (0,1/2,1/2) so is essentially the same as the simple atomic example described above. However, the two molecular sites have quite different orientations, since they are related by the  $2_1$ -screw axis of the space-group. Conventional structure determination reveals that the average structure is as shown in Figure 6a.

The shaded atoms are sites occupied by 50% Br and 50% methyl, and the whole average structure is very close to the space-group  $P2_1/c$  (although actually  $P2_1$ ). The  $2_1$ -screw axis is satisfied accurately, but the c-glide only approximately.

We now construct a model in which we replace the black and white atoms of Figure 5d,e,f with whole molecules of BEMB2 in their two different orientations A and B. The two different symmetry cases  $\Sigma_1$  and  $\Sigma_2$  take on a new significance. Instead of the lattice realization of Figure 5d consisting of small domains of atoms of all the same type, this is now replaced by regions of crystal in which the molecules are either all in the A orientation (black) or all in the B orientation (white). This corresponds to

regions of crystal in which the  $2_1$ -screw axis is maintained locally (see Figure 6b). Figure 5e, on the other hand, becomes a realisation in which the molecule at  $(0,1/2,1/2)$  tends to be of the opposite kind to that at  $(0,0,0)$ , and this corresponds to one in which there exists local domains satisfying the  $c$ -glide symmetry and not the  $2_1$ -screw axis (see Figure 6c).

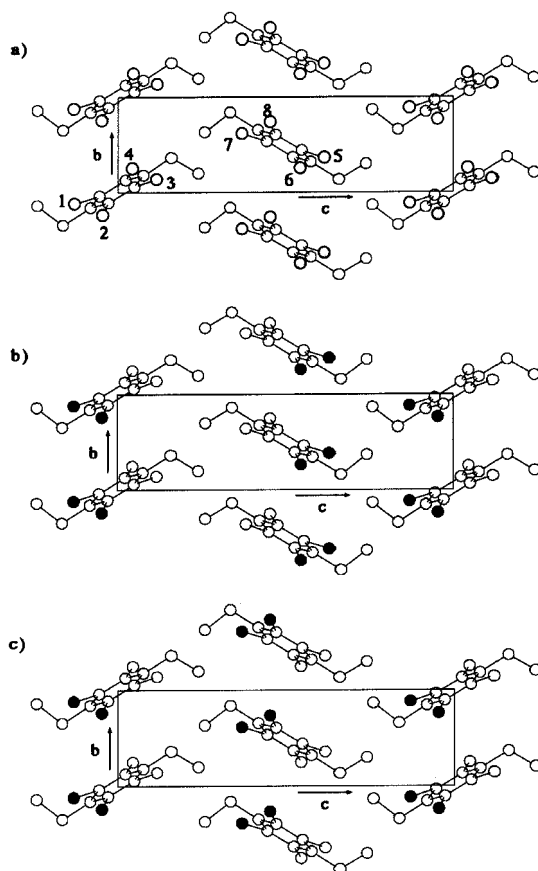


FIGURE 6. The structure of BEMB2 projected down the  $a$ -axis. a) the average structure (approx.  $P2_1/c$ ). b) The local structure ( $P2_1$ ) obtained when modulations are  $\Sigma_1$  symmetry. c) The local structure ( $Pc$ ) obtained when modulations are  $\Sigma_2$  symmetry.

In Figure 7a & 7b we show optical diffraction patterns obtained from these two realisations. It should be stressed that these two simulations contain exactly the same modulations as Figures 5a and 5b and the only things that have changed are that the atoms have been replaced by molecules, and the cell changed from a simple square to a rectangle appropriate to the  $a$ -axis projection of BEMB2. From these diffraction patterns it is clear that Figure 7b is a very good approximation to the observed X-ray pattern shown in Figure 2a and Figure 7a is quite wrong. This means that locally it is the c-glide symmetry that is satisfied and not the  $2_1$ -screw axis. Similar treatment of the  $(h\ k\ -h)$  section of BEMB2 leads to the same conclusion. In Figure 7c we show an optical diffraction pattern obtained using only  $\Sigma_2$  modes and the correspondence to Figure 2b is again very good.

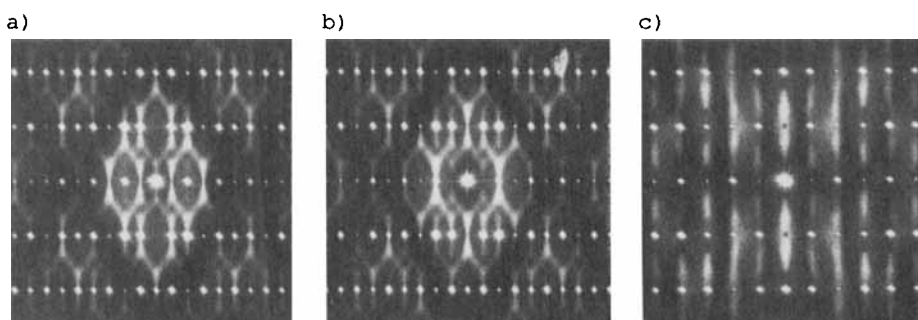


FIGURE 7. Optical diffraction patterns of BEMB2. 7a & 7b which correspond to the  $0kl$  section of BEMB2 were obtained by replacing the single atoms of Figures 5a & 5b with whole molecules in one or other of the two orientations A and B. For a) all modes are  $\Sigma_1$ . For b) all modes are  $\Sigma_2$ . 7c corresponds to the  $hk-h$  section and contains only modes of  $\Sigma_2$  symmetry. Note the 'hole' caused by the absence of modes close to  $k=0$ . Compare b) and c) with Figure 2.

These results appear to be in conflict with the observation from the crystal structure determination that in the average structure it is the  $2_1$ -screw axis that is satisfied and not the c-

glide. Now the structure determination corresponds to the average over a large volume of the structure and departures from the  $P2_1/c$  symmetry may be considered as modulations of wavevector  $k=0$ . That is to say, the fact that the average structure is  $P2_1$  rather than  $Pc$  means that the idealized  $P2_1/c$  structure is modulated by a  $k=0$  modulation of the  $\Sigma_1$  type while at wave vectors  $k \neq 0$  the modulations are entirely of the  $\Sigma_2$  type. I.e. one can imagine that there are two dispersion curve branches having the form shown schematically in Figure 8. Note that the 'hole' in the diffuse scattering in Figure 7c was obtained by omitting modulations close to  $k=0$ .

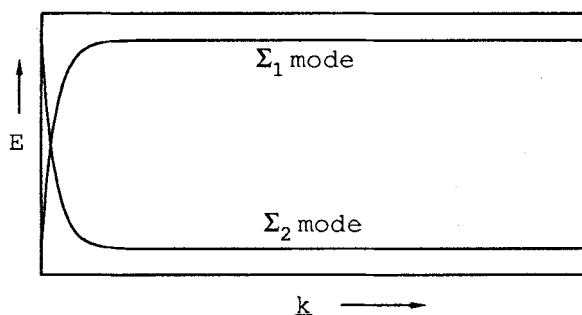


FIGURE 8. Schematic diagram showing the dispersion curves for the two compositional modulations  $\Sigma_1$  and  $\Sigma_2$ . Around the origin only modulations of  $\Sigma_1$  symmetry are excited; elsewhere it is those of  $\Sigma_2$  symmetry.

#### THE KITAIGORODSKY-WILSON THEORY OF CRYSTAL PACKING.

It is well known that organic molecules crystallize most frequently in a small number of space-groups. In fact the two space-groups  $P\bar{1}$  and  $P2_1/c$  account for about half of the entries in the Cambridge Structural Database<sup>12</sup>. Kitaigorodsky<sup>13</sup> explained this fact by asserting that these spacegroups were ones which permitted most readily the close-packing of triaxial ellipsoids. More recently Wilson<sup>14,15</sup> has extended these ideas by using the complimentary idea that space-group types are rare when they



contain symmetry elements - notably rotation axes and mirror planes - that prevent the molecules from freely choosing their positions within the unit cell, and has proposed an empirical relationship to express this. The frequency of occurrence of different space groups within the monoclinic system is given by:-

$$N_{sg} = A_{cc} \exp\left(-B_{cc}[2]_{sg} - C_{cc}[m]_{sg} - D_{cc}[\bar{1}]_{sg} - E_{cc}\right) \quad (6)$$

where  $N_{sg}$  is the number of occurrences of the space-group type,  $A_{cc}$  is a normalizing constant,  $[2]_{sg}$  is the number of twofold axes,  $[m]_{sg}$  is the number of mirror planes and  $[\bar{1}]_{sg}$  the number of inversion centres in one unit cell of the space-group type.  $B_{cc}$ ,  $C_{cc}$  and  $D_{cc}$  are parameters determined by fitting to the observed frequencies.  $E_{cc}$  is a constant dependent on the arithmetic class within the monoclinic system. In this form (6) the relative frequencies of occurrence of the monoclinic space-groups are accounted for quantitatively, with values of  $B_{cc}$ ,  $C_{cc}$  and  $D_{cc}$  of 6.41, 5.96 and 1.67 respectively. These values reflect the great impediment to close packing that 2-fold axes and m-planes impose, and a substantially lesser impediment imposed by a centre of symmetry.

The relevance of this to our present work is that this theory accounts for the fact that it is about 20 times more likely that a given molecule will prefer to crystallize in the space-group  $P2_1$  than in the space group  $Pc$  (the Cambridge data base contained 2488 and 133 entries respectively). It is therefore clear that, all other things being equal, the BEMB2 molecules would prefer to crystallize in the space-group  $P2_1$ , and this is indeed reflected in the *long-range order* that is observed.

Over a short range, however, things are very different and the molecules prefer to have a local arrangement more in keeping with the c-glide symmetry. This may be attributed to the dipole-dipole interactions between molecules. If we perform a simple experiment

in which we place dipoles at the molecular centres of a grid corresponding to the  $b$ - $c$  plane of Figure 6, it is found that the arrangement in which the dipoles are related by the  $c$ -glide is lower in energy than the arrangement in which they are related by the  $2_1$ -axis for all values of the angle  $\phi$  which the dipole makes with the  $b$ -axis.

#### REFERENCES.

1. T.R.Welberry, R.D.G.Jones and J.Epstein, Acta Cryst. **B38**, 1518 (1982).
2. J.Epstein, T.R.Welberry and R.D.G.Jones, Acta Cryst. **A38**, 611 (1982).
3. J.Epstein and T.R.Welberry, Acta Cryst. **A39**, 882 (1983).
4. T.R.Welberry and J.Siripitayananon, Acta Cryst. **B42**, 262 (1986).
5. T.R.Welberry and J.Siripitayananon, Acta Cryst. **B43**, 97 (1987).
6. J.C.Osborn and T.R.Welberry, J.Appl. Cryst. **23**, 476 (1990).
7. T.R.Welberry, Rep. Prog. Physics. **48**, 1543 (1985).
8. C.K.Johnson, ORTEPII. Report ORNL-5138. Oak Ridge National Laboratory, Tennessee. (1976).
9. T.R.Welberry R.L.Withers and J.C.Osborn, Acta Cryst. **B46**, 267 (1990).
10. T.R.Welberry and R.L.Withers, J.Appl. Cryst. **23**, 303 (1990).
11. C.J.Bradley and A.P.Cracknell, The Mathematical Theory of Symmetry in Solids, (Clarendon, Oxford, 1972).
12. F.H.Allen, S.Bellard, M.D.Brice, B.A.Cartwright, A.Doubleday, H.Higgs, T.Hummelink, B.G.Hummelink-Peters, O.Kennard, W.D.S.Motherwell, J.R.Rodgers and D.G.Watson, Acta Cryst. **B35**, 2331 (1979).
13. A.I.Kitaigorodsky, Molecular Crystals and Molecules, (Academic Press, New York, 1973).
14. A.J.C.Wilson, Acta Cryst. **A44**, 715 (1988).
15. A.J.C.Wilson, Acta Cryst. **A46**, 742 (1990).